Beam Based Alignment Using a Neural Network*

Guanliang Wang,[1] Kemin Chen,[1] Siwei Wang,[2] Zhe Wang,[1] Tao He,[1] Masahito Hosaka,[1] Guangyao Feng,[1] and Wei Xu[1,†]

[1]*National Synchrotron Radiation Laboratory, University of Science and Technology of China, Hefei, Anhui 230029, China*

[2]*Diamond Light Source, Oxfordshire OX11 0DE, United Kingdom*

Beams usually do not travel through the magnet centers due to errors in storage rings. The beam deviating from the quadrupole centers is affected by additional dipole fields due to magnetic field feed-down. The beam-based alignment (BBA) is often performed to find a golden orbit, on which the beam circulates around the quadrupole center axes. For storage rings with a large number of quadrupoles, the conventional BBA procedure is time-consuming, especially in the commissioning phase due to the necessary iterative process. Additionally, the conventional BBA method can be affected by strong coupling and nonlinearity of the storage ring optics. In this work, a novel method based on a neural network is proposed to find the golden orbit in a much shorter time with reasonable accuracy. This golden orbit can be directly used for operation, or can be adopted as the starting point for the conventional BBA. The method is demonstrated in the HLS-II storage ring for the first time, through simulation and online experiments. The results of the experiments show that the golden orbit obtained using this new method is consistent with that from the conventional BBA. The development of this new method and corresponding experiments are reported in this paper.

Keywords: Golden orbit, Beam-based alignment, Neural network, Storage ring.

I. INTRODUCTION

Ideally, the beam in a storage ring should circulate on the orbit passing through the axes of all magnet centers, which is called the golden orbit. The beam orbit may deviate from the ideal path due to various errors, such as misalignment, magnet imperfection, power regulation errors, etc. When the beam traverses the magnets with orbit offsets, it will see undesired magnetic fields which is called feed-down [1]. The feed-down of a quadrupole with an orbit offset causes an additional dipole field. To minimize this effect, the beam-based alignment can be adopted to determine the golden orbit for machine operation. It has been widely used in the commissioning of storage rings [2, 3]. For storage rings with long circumference, such as most diffraction-limited storage rings (DLSRs), the number of quadrupoles is large and the conventional BBA method becomes much time-consuming [4]. Recently a fast BBA method is developed in the ALBA light source using AC excitation of the orbit correctors and fast beam position data acquisition [5–7]. At HLS-II, with no need to upgrade the hardware, a machine learning (ML) based method is developed to find the golden orbit for storage rings[8].

Neural networks (NNs) have been widely applied in artificial intelligence and have gained great success in various fields. Its application has also been introduced to the area of particle accelerators [9–12]. At Advanced Light Source (ALS), an NN model is used to maintain the vertical beam size when the gap of insertion devices varies [13]. The NN model can also be used to greatly reduce the simulation time for the optimization of beam dynamics [14]. At Shanghai Synchrotron Radiation Facility (SSRF), the image processing technique using convolutional neural networks (CNNs) is adopted to extract bunch longitudinal phase information [15]. These applications show great potential of NNs in improving accelerator performances.

In this paper, we present a new BBA method that uses an NN model to predict the golden orbit of a storage ring. To initiate the experiment, different closed orbits are generated by randomly changing the strength of all orbit correctors. The beam with various orbit deviations in the quadrupoles is subject to various amount of influence from their feed-down. This effect can be evaluated by measuring the orbit change caused by quadrupole strength variation. Since the beam on the ideal golden orbit should not be disturbed by changing the quadrupole strength, an NN model can then be trained to search for the orbit that is least affected by varying quadrupole strength. To train this model, the orbit differences due to quadrupole change is used as the input data, and the corresponding orbits before quadrupole adjustment is used as the output data. The golden orbit is then predicted by setting the input value as zero to the NN model.

The new BBA method is tested in the HLS-II storage ring through simulation and online experiments to demonstrate its validity. The result shows that the golden orbit obtained from the NN model is consistent with that obtained by several iterations with the conventional method. The golden orbit obtained using this method can be directly used for operation or used as a starting point to speed up the conventional BBA that requires several iterations. In general, this new method is less time-consuming compared to the conventional BBA especially in the case during the initial commissioning [16].

In the following sections, the methods of the conventional BBA and the new BBA using an NN model are shown in Section II. The simulated result using these two BBA methods in the HLS-II storage ring is described in Section III. The online experiments using both BBA methods are introduced in Section IV. Finally the work is summarized in Section V.

* This work was supported by the National Natural Science Foundation of China under Grant 11975227.

† wxu@ustc.edu.cn

II. BEAM-BASED ALIGNMENT

A. Conventional BBA method

The purpose of the BBA is to find a reference orbit in which the beam passes the centers of all quadrupoles in a storage ring using beam position monitors (BPMs) and orbit corrector magnets (OCMs). A quadrupole generates dipole fields with strengths

$$B_x = B_0\rho_0 K_0 y_0, \tag{1}$$
$$B_y = B_0\rho_0 K_0 x_0, \tag{2}$$

where $B_0\rho_0$ is the magnetic rigidity, K_0 is the normalized quadrupole strength, x_0 and y_0 are the beam offsets relative to the quadrupole center in the horizontal and vertical plane, respectively. Therefore, changing the quadrupole strength by ΔK causes a dipole field variation by

$$\Delta B_x = B_0\rho_0 \Delta K y_0, \tag{3}$$
$$\Delta B_y = B_0\rho_0 \Delta K x_0, \tag{4}$$

resulting in a kick which leads to an orbit change at an observation point s by [17]

$$\begin{aligned}\Delta\boldsymbol{u}(s) = \Delta K \boldsymbol{u}(s_0)\left(\frac{1}{1 - K_0\frac{L_0\beta(s_0)}{2\tan(\pi\nu)}}\right)\\ \times\frac{\sqrt{\beta(s)\beta(s_0)}}{2\sin(\pi\nu)}\cos(|\phi(s)-\phi(s_0)|-\pi\nu),\end{aligned} \tag{5}$$

where L_0 is the length of the quadrupole, ν is the betatron tune, $\beta(s_0)$ and $\beta(s)$ are the beta functions at the locations of the quadrupole and observation point respectively, $\phi(s_0)$ and $\phi(s)$ are the phase advances at the locations of the quadrupole and observation point and $\boldsymbol{u}$ stands for the beam positions in the horizontal and vertical plane. This equation shows that the beam orbit can be affected by the quadrupole strength variation and also the beam positions in the quadrupoles. To avoid this effect, the reference orbit of the orbit feedback system is usually set to the centers of all quadrupoles with $\boldsymbol{u} = \boldsymbol{0}$. This reference orbit can be determined using the BBA technique.

The quadrupole center is measured using its nearest BPM. Suppose that when the beam goes through the quadrupole center, the related reading of this BPM is $\boldsymbol{v}_0$. According to Eq. (5), by changing the quadrupole strength ΔK, the beam orbit change is given by

$$\Delta\boldsymbol{u} = \Delta K \mathcal{F}(\boldsymbol{v} - \boldsymbol{v}_0), \tag{6}$$

where $\boldsymbol{v}$ is the reading of the target BPM before quadrupole strength change and $\mathcal{F}$ is the coefficient which can be easily obtained from Eq. (5). To measure the quadrupole center, the beam is set to several difference positions at its related BPM. For each position, the quadrupole strength is then changed with the same ΔK and the corresponding orbit change is recorded. By applying a linear fit to Eq. (6), the quadrupole center $\boldsymbol{v}_0$ is obtained. This conventional BBA always determines the horizontal and vertical offsets separately [18]. The above analysis implies that the coefficient $\mathcal{F}$ is treated as a constant, which means the beam optics remain unchanged during BBA process. In fact, the change of quadrupole strength and the closed orbit distortion can affect the beam optics. At the beginning of commissioning, the beam orbit and beam optics are possibly far different from the ideal model which induces strong nonlinearity and coupling. In this case, it needs several iterations for the conventional BBA method to eliminate the nonlinear effects and obtain more accurate quadrupole centers. A neural network with multi-layers which deals with nonlinear problems can be adopted for the BBA process [19, 20].

B. BBA using a neural network

BBA is based on the principle that the off-axis beam is affected by the quadrupole strength change. The golden orbit can then be evaluated using the relation between the orbit changes and the initial beam orbits before varying the quadrupole strength. This relation can be explored by training a neural network using the orbit changes as the input data and the initial orbits as the output data. By setting the orbit change to zero, the corresponding initial beam orbit is just the predicted golden orbit. The main idea of this new BBA method is shown in Fig. 1. To obtain data for training the NN model, the simulation or online experiment is carried out as follows:

- Randomly exciting all corrector magnets to form a initial closed orbit;
- Recording all BPM readings;
- Changing all quadrupoles with a same amount to form a new closed orbit.
- Recording the changes in all BPM readings;
- Resuming the quadrupole and corrector strengths to the original values;
- Repeating the above procedures.

A typical dense neural network has one input layer, several hidden layers (also called middle layers), and one output layer, as shown in Fig. 2 [21]. The nodes are called neurons where the data are transferred. The nodes between adjacent layers are connected to each other by an arrow, which shows the flow of data. Each arrow represents a linear transformation combined with an activation function used to introduce nonlinearity if necessary [11]. A loss function is used to describe the performance of the neural network. The NN also needs an optimizer function to optimize the parameters used for data transmission. The optimization is carried out by minimizing the loss value.

III. SIMULATION STUDY FOR THE HLS-II STORAGE RING

Simulation is carried out to evaluate the validity of the new BBA method based on an NN model before online experi-

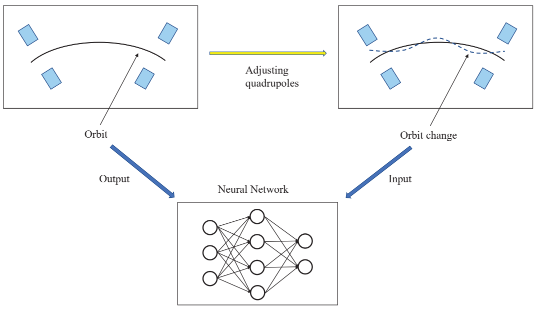

Fig. 1. Schematic of the neural network based BBA method. Different orbits are generated by randomly adjusting the orbit correctors. On each orbit, all quadrupoles are changed with the same ΔK at the same time to generate orbit changes. The orbit changes are used as the input data of the neural network and the corresponding initial orbits are used as the output data for the training.

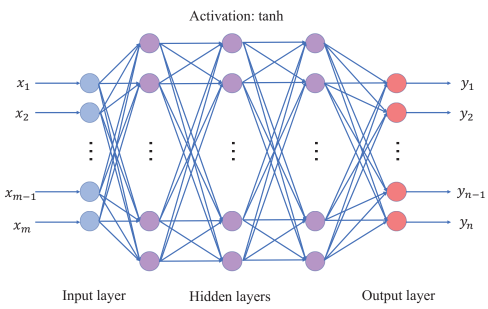

Fig. 2. Diagram of a typical dense neural network, which consists of one input layer, several hidden layers and one output layer. Here hyperbolic tangent $(\tanh)$ is adopted as the activation function.

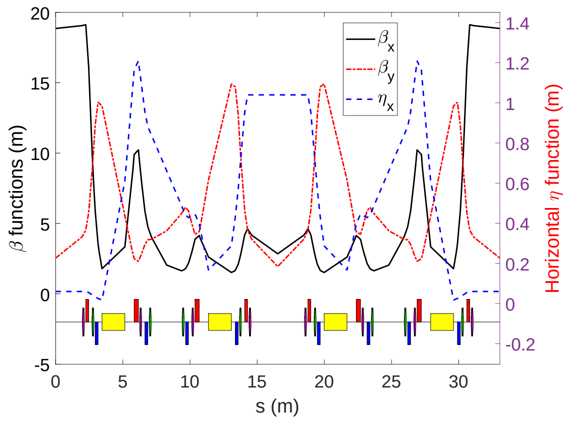

Fig. 3. One super period of the HLS-II lattice. There are 32 quadrupoles and 32 BPMs in the storage ring. The 32 combined-function sextupoles are used as the horizontal and vertical correctors.

Table 1. Misalignment error settings used for the HLS-II storage ring.

Type	Shift error (μm)			Rotation error (μrad)		
Axis	X	Y	S	X	Y	S
Girder	50	50	200	500	500	500
Dipole	200	200	150	500	500	500
Quadrupole	200	200	150	500	500	500
Sextupole	200	200	150	500	500	500
BPM	200	200	150	500	500	500

ments. The accelerator toolbox (AT) is used for the simulation in this work [22]. TensorFlow, which is adopted in this work, provides a flexible platform that makes it easy for users to build and train an NN model [23, 24].

The HLS-II storage ring has two super periods with a circumference of $66.1\,\mathrm{m}$. The layout for one super period is shown in Fig. 3. The orbit system of the storage ring consists of 32 BPMs and 32 correctors combined to the sextupoles. 32 quadrupoles are installed which need to measure their real centers through the BBA procedure [25].

Random rotation and shift errors are applied to simulate the misalignment of the elements and girders. The errors are generated in a normal distribution with truncation at three standard deviations. According to the design report, the error settings of all magnets, girders and BPMs are listed in Table 1. A set of misalignment errors of the whole ring is shown in Table 4. The magnet strength errors are also applied. The BPM random measurement error is set as $0.5\ \mu\mathrm{m}$ [26].

A. Conventional BBA method

In the conventional BBA measurement for one quadrupole, the beam is moved to three different positions with the help of the corrector magnets [27]. At each position, the change in the beam orbit from all BPM readings is recorded after varying the strength of the target quadrupole with a certain ΔK. The orbit changes can be fitted linearly as a function of the beam position in the target quadrupole. An immobile point can be found by setting the position at which the BPM changes vanish. The quadrupole center is then obtained by adding up all immobile points from each BPM. A whole BBA routine repeats this process for all quadrupoles in both horizontal and vertical planes in the storage ring. To increase the BBA accuracy, one can repeat the measurement after moving the beam to the orbit obtained from the previous BBA experiment. This scheme is usually needed at the machine commissioning stage. Fig. 5 shows the simulated measurement of the horizontal and vertical centers of one quadrupole magnet in the HLS-II storage ring. At least three conventional BBA iterations are needed to decrease the standard deviation of the fitted Gaussion function of the quadrupole center to several microns, which is the same order of BPM measurement resolution [28].

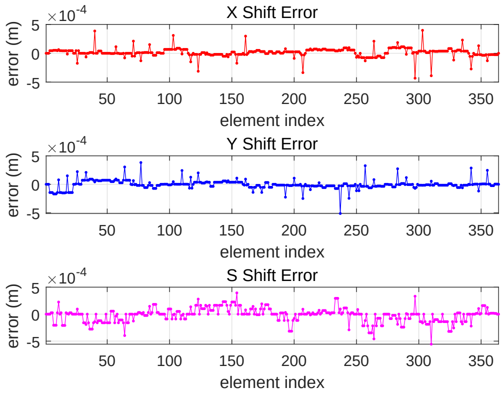

(a) Shift error

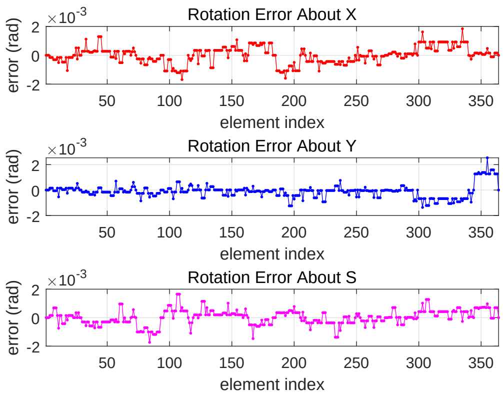

(b) Rotation error

Fig. 4. Misalignment errors applied to the HLS-II storage ring. (a) Shift errors. (b) Rotation errors.

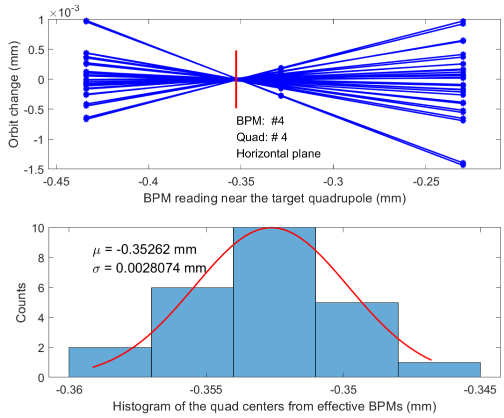

(a) The horizontal plane

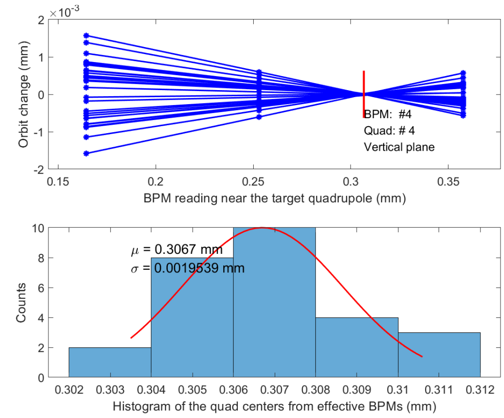

(b) The vertical plane

Fig. 5. Simulated BBA measurement in the HLS-II storage ring. The horizontal and vertical measurement is applied respectively. (a) Horizontal quadrupole center measurement. (b) Vertical qadrupole center measurement. The plots show the orbit change observed from all BPMs by varying the target quadrupole strength with a certain ΔK when the beam is at three different positions. For each BPM, its changes can be fitted to find a center for the quadrupole. All of the found centers are then fitted using the Gaussian function. The red line shows the fitted centers using all BPMs, which represents the BBA center of this quadrupole.

B. BBA using an NN model

In the simulation, the correctors are set randomly with a certain range kicks to move the beam orbit. Here, the kick angle variations are generated by a normal distribution with the standard deviation of $0.05\,\mathrm{mrad}$ and a truncation at three standard deviations is applied. For each random orbit, all quadrupoles are simultaneously changed with a same amount of ΔK ($-0.02\,\mathrm{m}^{-2}$). The corresponding initial beam orbit and orbit changes are recorded from all BPMs.

The whole simulation generates 10000 samples. In each sample, there are 64 initial orbits and 64 orbit change data, with 32 in the horizontal plane and 32 in the vertical plane. These samples are adopted for training the neural network. Fig. 6 shows the random initial beam orbits within a range of $(-5, 5)$ mm. Fig. 7 shows the orbit change after the quadrupole adjustment. The range of orbit change is within $(-1.5, 1.3)$ mm and $(-0.8, 0.8)$ mm in the horizontal and vertical plane, respectively.

To obtain the golden orbit, an NN model is trained using these data. The 64 sets of orbit change data are set as the input of the model, and the 64 sets of the corresponding initial orbit data are set as the output of the model. 80% of the data are used to train the model and the rest are used to test the performance of the model. There are 128, 256 and 128 neurons in the three hidden layer, respectively. The $\tanh$ is taken as the activation function to provide nonlinearity. The NN model is trained using the Adam optimizer [29]. The loss function is the mean squared error (MSE) between the measured data and model-predicted result, which is

$$\text{loss} = \text{mean}((\mathbf{r}_{\text{model}} - \mathbf{r}_{\text{real}})^2). \tag{7}$$

Fig. 8 shows the comparison of the golden orbits obtained from the conventional BBA and the BBA using a neural network. The good consistency of these two BBA methods

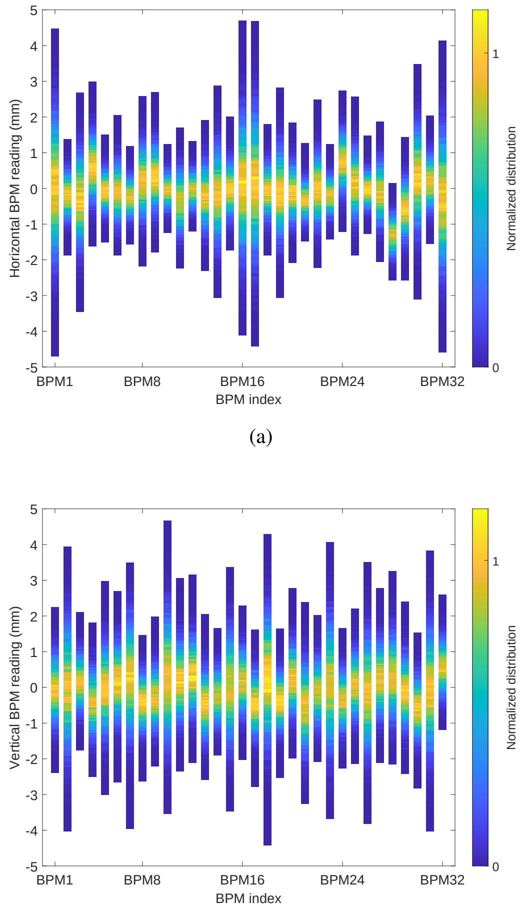

(a)

(b)

Fig. 6. Distribution of the initial orbits generated by randomly adjusting the orbit correctors within a certain range. (a) Initial orbits in the horizontal plane. (b) Initial orbits in the vertical plane.

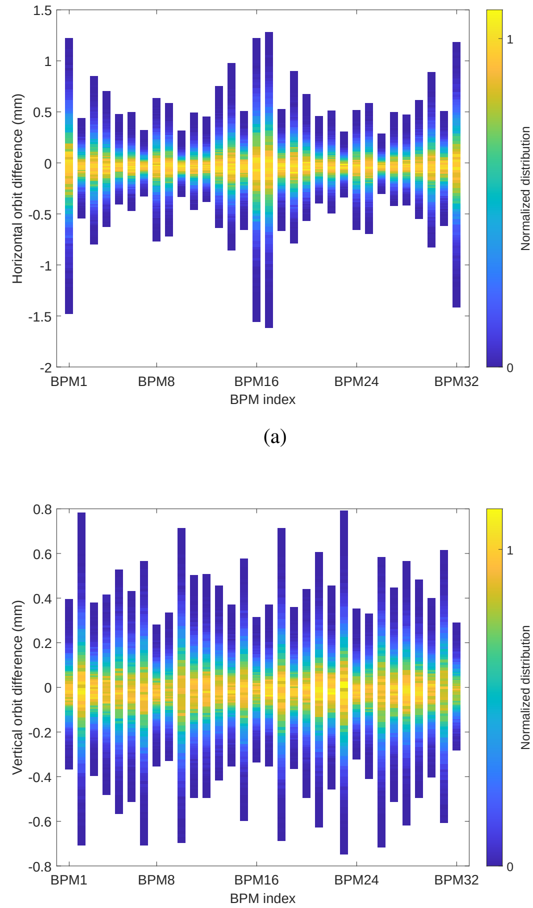

(a)

(b)

Fig. 7. Distribution of orbit change caused by varying the quadrupole strength for each random orbit in the simulation. (a) Horizontal orbit changes. (b) Vertical orbit changes.

shows the validity and effectiveness of this new BBA technique. Next the online experiment is carried out in the HLS-II storage ring.

IV. ONLINE EXPERIMENT IN THE HLS-II STORAGE RING

The conventional BBA has been applied to the HLS-II storage ring [30]. Fig. 9 shows the BBA result for one quadrupole. The errors of fitting for most quadrupoles are within 20 μm.

A. Training data acquisition

Similar to the simulation, the training data could be obtained from the real storage ring. Before experiment, the magnet strengths are set according to the result from the early commissioning of the storage ring. In this case, the beam

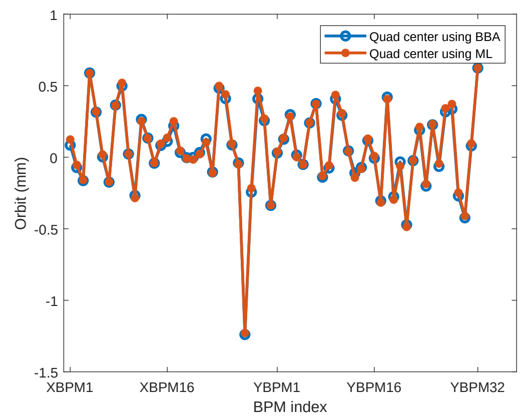

(a) Quadrupole centers

Fig. 8. The quadrupoles centers obtained from the conventional BBA and the NN-based BBA. The simulation shows good consistency of these two methods.

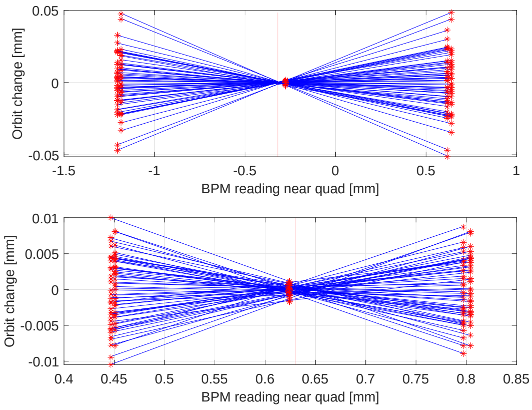

Fig. 9. Measurement of BBA for one quadrupole in the HLS-II storage ring. The upper and lower plots show the horizontal and vertical orbit changes observed from all BPMs by varying the target quadrupole strength with a certain ΔK when the beam is at three different positions. For each BPM, the change in its reading can be fitted to find a center for the quadrupole. The red line shows the averaged fitted centers using all BPMs, which represents the BBA center of this quadrupole.

is not on the golden orbit which connects the centers of the quadrupoles. The online experiment for obtaining training data is reported in this subsection.

During the online experiment, the orbit feedback system is turned off and the correctors are randomly set to generate different orbits. As a compromise of beam stability and data diversity, the adjustment range of all correctors is set to $\pm 0.8\,\mathrm{A}$ relative to the starting point. This adjustment range of correctors ensures no beam loss during the experiment by controlling the orbit change within a distinguishable range, as shown in Fig. 10. The horizontal tune in the HLS-II storage ring is about 4.44 while the vertical tune is 2.36 which is further from the half-integer. When the quadrupole strength is increased simultaneously, the horizontal tune increases and easily reaches the half-integer resonance and causes beam loss. Therefore, all quadrupoles strength is adjusted in the decreasing direction, by an amount of $-0.02\,\mathrm{m}^{-2}$ (normalized focusing strength). After the orbit change is recorded, all quadrupole strength is restored to the original values. For the HLS-II storage ring, the time constant for the orbit corrector power supplies is about $15\,\mathrm{ms}$ [30]. The time constant for the quadrupole power supplies is about $30\,\mathrm{ms}$. This means that one complete loop of this measurement could be done within 1 second. To ensure the accuracy of the data acquisition, the measurement time for one loop is set to 2 seconds.

The online experiment is carried out during the machine study time [31]. The whole measurement generates 21000 samples. These samples are adopted for training the neural network. Fig. 10 shows the randomly generated initial beam orbits before varying the quadrupole strength. The distribution shows that the orbits are generated within the range of about (-10,10) mm, and the densest distribution is around 0. The orbit change after the quadrupole adjustment is also analyzed, and the distribution of the orbit differences is plotted in Fig. 11. The range of orbit change is within (-3,2) mm in the horizontal plane and within (-1.5,1.5) mm in the vertical plane.

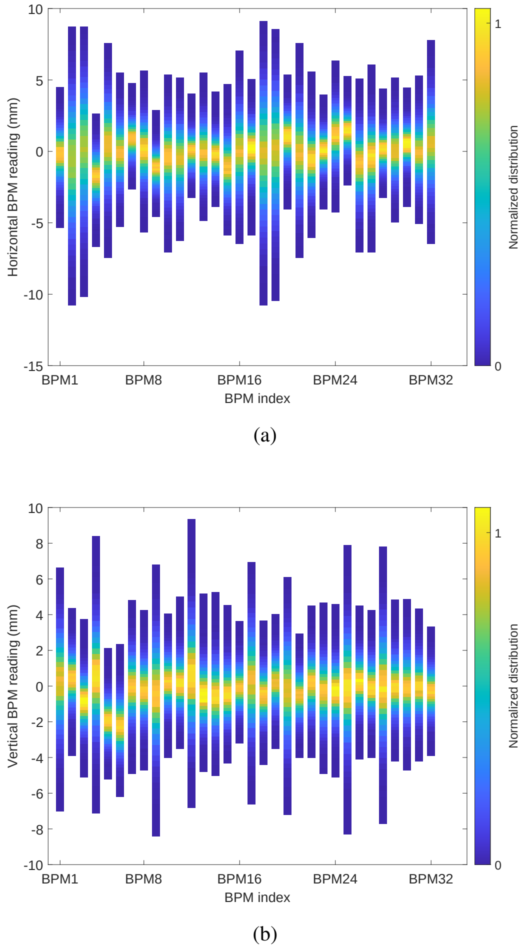

Fig. 10. Distribution of the orbits generated by randomly adjusting the orbit correctors within a certain range. (a) Horizontal BPM readings. (b) Vertical BPM readings.

B. NN model training using online data

In this subsection, the relation between the initial orbit and orbit change after quadrupole adjustment is explored using a dense neural network. Similar to the simulation, the 64 sets of the orbit change data are set as the input to the model, and the 64 sets of the corresponding initial orbit data are set as the output of the model. To figure out the data size requirement, two models are trained with different numbers of samples. In model I, all 21000 samples are adopted, 5/6 of the samples are used for training, and 1/6 are the validation data set. As a comparison, model II is trained with only 3000 samples in the training set and 600 samples in the validation set, namely 3600 samples are adopted in total. The Adam optimizer and

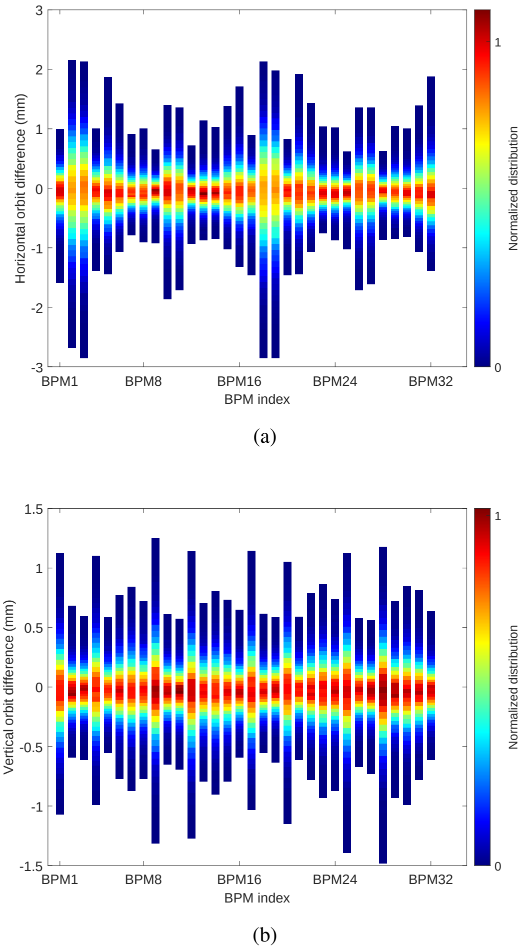

Fig. 11. Distribution of orbit change after varying the quadrupoles for each random orbit. (a) Horizontal orbit change. (b) Vertical orbit change.

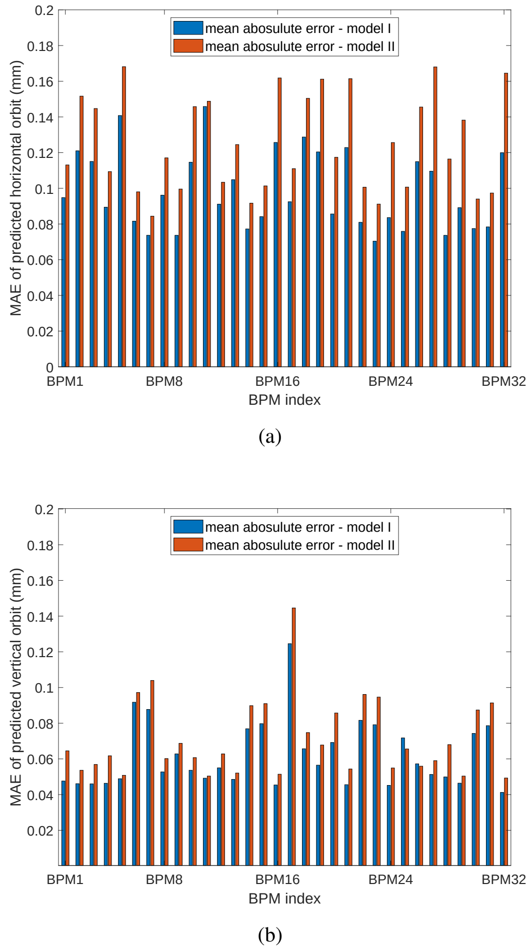

Fig. 12. The mean absolute error (MAE) between the measured beam orbits and predicted values of the validation samples for all BPMs. (a) Horizontal plane. (b) Vertical plane.

the MSE loss function are used for training models.

The trained NN models are evaluated by calculating the mean absolute error (MAE) between the measured real values and model-predicted values of the validation samples for each BPM:

$$\mathrm{MAE} = \mathrm{mean}(|\mathbf{r}_{\mathrm{measured}} - \mathbf{r}_{\mathrm{predicted}}|). \tag{8}$$

The absolute error for both models is shown in Fig. 12, which shows that the errors of model I are smaller than those of model II. In the horizontal plane, the overall averaged absolute error is around 99 μm for model I and 125 μm for model II. In the vertical plane, the overall averaged absolute error is around 62 μm for model I and 71 μm for model II. The result shows that increasing samples for the NN model training can improve the model accuracy.

C. Golden orbit from the NN model

In the NN training, the orbit changes caused by varying the quadrupoles are used as the input data. The corresponding initial orbits are used as the output data. The beam on the golden orbit should have the least orbit distortion (ideally zero) due to the change in quadrupole strength. Therefore, we can set the input as zero to the NN model and the corresponding output is just the golden orbit.

To estimate its accuracy, this golden orbit is compared with that obtained using the conventional BBA method and the result is shown in Fig. 13. The sub-figures in Fig. 13 show the difference between the novel and conventional BBA. The result shows that this golden orbit is consistent with that obtained from the conventional BBA. In the horizontal plane, the averaged difference between the conventional BBA and the model prediction is around 46 μm for model I and 53 μm for model II. In the vertical plane, the averaged difference between the conventional BBA and the model prediction is around 42 μm for model I and 39 μm for model II.

Although the training error of model I is obviously smaller than that of model II, the difference in the predicted golden orbits from these two models does not have a large deviation [32]. In the HLS-II storage ring, the typical experimental

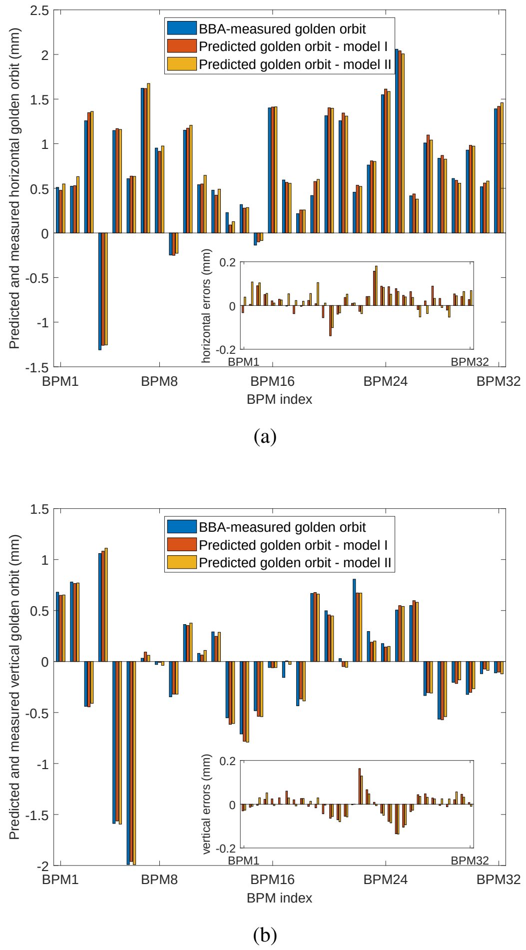

Fig. 13. Comparison of the golden orbit obtained using the NN model and the conventional BBA method. The difference between the two golden orbits is shown in the subfigure. (a) Horizontal golden orbit. (b) Vertical golden orbit.

period for the conventional BBA process is around 5 hours. In the machine commissioning phase, this BBA process needs to be repeated several times to obtain a precise result. Model II uses only 3600 samples, which leads to a shorter online measurement time (about 2 hours). As discussed above, the online measurement time for this new method is irrelevant to the total quadrupole number. This differs from the conventional BBA where the larger the storage ring, the more time it takes. On the other hand, the NN trained golden orbit can be set as the starting point for the conventional BBA. This helps to reduce the iterative process of the BBA starting from the initial commissioning orbit and hence the experimental time.

V. SUMMARY

A novel method is developed to search for the golden orbit of a storage ring. This method trains a neural network model using the simulated or online data of different closed orbits and the corresponding orbit change caused by varying all quadrupole strength simultaneously. The online experiment can be done with less time especially for large storage rings. This golden orbit is compared with the one obtained using conventional BBA and the result shows good consistency.

The NN-based BBA is a good choice for the commissioning stage of a storage ring where the beam optics is far different from the ideal model and the closed orbit is deviated from the magnet centers. In this case, the linear process of the conventional BBA is not accurate anymore. Besides, the conventional BBA treats the horizontal and vertical orbits separately. However, the coupling of a real machine is non-negligible especially when the coupling is not sufficiently corrected. The NN-based method deals with the transverse planes simultaneously which naturally solves the coupling issue. Additionally, the new BBA method can be better applied to storage rings with strong nonlinear effects, which is often the case for DLSRs. With strong nonlinearity, the conventional BBA method might work within a limited region since the linearity of the orbit response is assumed. Since the NNs can be used to solve nonlinear problems as is well known, this NN-based BBA method is expected to work more effectively for the DLSRs. In another perspective, this new technique can better deal with the cases where the quadrupoles are powered in series, since there is no need to vary the strength of all quadrupoles individually. It is anticipated that some small light sources or boosters will be benefited from this new BBA method.

ACKNOWLEDGMENT

The authors would like to thank the engineers and scientists at HLS-II for their valuable suggestions and assistance in the machine studies.

[1] X.B. Huang, Simultaneous beam-based alignment measurement for multiple magnets by correcting induced orbit shift. PHYS. REV. ACCEL. BEAMS (2022). doi: 10.1103/PhysRevAccelBeams.25.052802

[2] M. Aiba, M. Böge, H. Braun et al., Study of beam based alignment and orbit feedback for SwissFEL. Proc. of FEL10.

[3] A. Madur, P. Brunelle, A. Nadji et al., Beam based alignment for the storage ring multipoles of synchrotron SOLEIL. Proceedings of EPAC.

[4] Y. Zhao, Y. Jiao, S. Wang, Design study of APS-U-type hybrid-MBA lattice for mid-energy DLSR. Nucl. Sci. Tech. (2021). doi: 10.1007/s41365-021-00902-1

[5] Z. Martí, G. Benedetti, M. Carlà et al., Fast orbit response matrix measurements at ALBA. 8th Int. Particle Accelerator Conf. (IPAC'17), Copenhagen, Denmark, 14 19 May, 2017.

[6] Z. Martí, G. Benedetti, U. Iriso et al., Fast quadrupole beam based alignment using AC corrector excitations. 9th Int. Particle Accelerator Conf. (IPAC'18), Vancouver, BC, Canada, April 29-May 4, 2018.

[7] Z. Martí, G. Benedetti, U. Iriso et al., Fast beam-based alignment using AC excitations. PHYS. REV. ACCEL. BEAMS (2020). doi: 10.1103/PhysRevAccelBeams.23.012802

[8] Z.H. Zhou, Machine learning.

[9] A. Edelen, N. Neveu, M. Frey et al., Machine learning for orders of magnitude speedup in multiobjective optimization of particle accelerator systems. PHYS. REV. ACCEL. BEAMS (2020). doi: 10.1103/PhysRevAccelBeams.23.044601

[10] J.Y. Wan, P. Chu, Y. Jiao et al., Improvement of machine learning enhanced genetic algorithm for nonlinear beam dynamics optimization. NUCL. INSTRUM. METH. A (2019). doi: 10.1016/j.nima.2019.162683

[11] J.Y. Wan, P. Chu, Y. Jiao, Neural network-based multiobjective optimization algorithm for nonlinear beam dynamics, PHYS. REV. ACCEL. BEAMS (2020). doi: 10.1103/PhysRevAccelBeams.23.081601

[12] Y.B. Yu, G.F. Liu, W. Xu et al., Research on tune feedback of the Hefei Light Source II based on machine learning. Nucl. Sci. Tech. (2022). doi: 10.1007/s41365-022-01018-w

[13] S.C. Leemann, S. Liu, A. Hexemer et al., Demonstration of machine learning-based model-independent stabilization of source properties in synchrotron light sources. PHYS. REV. LETT. (2019). doi: 10.1103/PhysRevLett.123.194801

[14] Y.J. Li, W.X. Cheng, L.H. Yu et al., Genetic algorithm enhanced by machine learning in dynamic aperture optimization. PHYS. REV. ACCEL. BEAMS (2018). doi: 10.1103/PhysRevAccelBeams.21.054601

[15] X.Y. Xu, Y.M. Zhou, Y.B. Leng, Machine learning based image processing technology application in bunch longitudinal phase information extraction. PHYS. REV. ACCEL. BEAMS (2020). doi: 10.1103/PhysRevAccelBeams.23.032805

[16] P. Raimondi, N. Carmignani, L.R. Carver et al., Commissioning of the hybrid multibend achromat lattice at the European Synchrotron Radiation Facility. PHYS. REV. ACCEL. BEAMS (2021). doi: 10.1103/PhysRevAccelBeams.24.110701

[17] J. Niedziela, C. Montag, T. Satogata, Quadrupole beam-based alignment at RHIC. Proceedings of the 2005 Particle Accelerator Conference.

[18] X.B. Huang, Beam-based correction and optimization for accelerators.

[19] S. Grossberg, Nonlinear neural networks: Principles, mechanisms, and architectures. Neural networks (1988).

[20] V.Y. Kreinovich, Nonlinear neural networks: Principles, mechanisms, and architectures. Neural networks (1991). doi: 10.1016/0893-6080(91)90074-F

[21] C.M. Bishop, Neural networks and their applications. Review of scientific instruments (1994).

[22] A. Terebilo, Accelerator toolbox for MATLAB. SLAC National Accelerator Lab., Menlo Park, CA (United States) (2011).

[23] B. Pang, E. Nijkamp, Y.N. Wu, Deep learning with tensorflow: A review. Journal of Educational and Behavioral Statistics (2020). doi: 10.3102/1076998619872761

[24] M. Abadi, A. Agarwal, P. Barham et al., Tensorflow: Large-scale machine learning on heterogeneous distributed systems[J]. arXiv preprint (2016). 10.48550/arXiv.1603.04467

[25] Z.H. Bai, L. Wang, Q.K. Jia et al., Lattice study for the HLS-II storage ring. CHINESE. PHYS. C (2013). doi: 10.1088/1674-1137/37/4/047004

[26] F.F. Wu, Y.L. Yang, B.G. Sun et al., Introduction of beam position monitor system in the HLS II storage ring. 8th Int. Particle Accelerator Conf. (IPAC'17), Copenhagen, Denmark, 14 19 May, 2017.

[27] V. Kiselev, V. Smaluk, Measurement of local impedance by an orbit bump method. NUCL. INSTRUM. METH. A (2004). doi: 10.1016/j.nima.2004.01.077

[28] J.S. Cao, L. M, H.Z. Ma et al., Application of Libera BPM at BEPC II for the early commissioning. CHINESE. PHYS. C (2008).

[29] Z.J. Zhang, Improved Adam optimizer for deep neural networks. 2018 IEEE/ACM 26th International Symposium on Quality of Service (IWQoS).

[30] W. Xu, J.Y. Li, K. Xuan et al., Orbit stabilization for the HLS-II storage ring. 9th Int. 7th Int. Particle Accelerator Conf. (IPAC'16), Busan, Korea, May 8-13, 2016.

[31] J.Y. Li, W. Xu, K. Xuan, Operation status of HLS-II. THPOY028, IPAC16.

[32] G.L. Wang, S.W. Wang, K.M. Chen et al., Beam reference orbit compensation for the HLS-II storage ring. J. INSTRUM. (2023). doi: 10.1088/1748-0221/18/06/T06004